J Membrane Biol (2009) 227:57–66
DOI 10.1007/s00232-008-9143-3

ORIGINAL ARTICLES

Involvement of Amino Acid 36 in TM1 in Voltage Sensitivity in Mouse Na^+/Glucose Cotransporter SGLT1

Ana Díez-Sampedro

Received: 18 August 2008 / Accepted: 22 November 2008 / Published online: 3 January 2009

Abstract Human SGLT1 protein is an established sodium-glucose cotransporter. Despite widespread use of the mouse as a model organism, the mouse SGLT1 homologue has yet to be functionally characterized. Additionally, the crystal structure of a sugar transporter homologue, *Vibrio* SGLT, has recently been described, however, it offers limited information about the role of transmembrane segments outside of the core ligand binding domains. In particular, the amino acids in TM1 were not assigned in the structure. To examine the contribution of TM1 to the function of SGLT1, we have cloned and characterized the biophysical properties of SGLT1 from mouse, mSGLT1, and compared it to a clone containing an amino acid substitution in TM1, F36S. As predicted, both proteins formed functional Na^+/sugar cotransporters, but F36S-mSGLT1 showed decreased rates of sugar uptake and decreased apparent affinities for both Na^+ and sugar compared to mSGLT1. Analysis of pre-steady-state currents and comparison with the crystal structure of *Vibrio* SGLT provide plausible mechanisms to explain the differences in function of these two proteins. Our data suggest that amino acids in TM1, which are not involved in ligand binding and translocation pathways, significantly influence the functional properties of sodium-glucose carrier proteins.

Keywords Na^+/glucose cotransporter · SGLT1 · Mouse · Solute carrier

A. Díez-Sampedro (✉)
Department of Physiology and Biophysics, University of Miami, School of Medicine, Miami, FL 33136, USA
e-mail: adiezsampedro@med.miami.edu

Introduction

The human sodium-glucose cotransporter type 1 (hSGLT1) protein is a member of a large family of solute transporters. It is best known for its role in transporting glucose across the intestinal brush border using the transmembrane sodium electrochemical gradient (Kimmich 1981). Murine models of intestinal function are well established for their functional significance and the mouse has become a popular model organism in science. As an example, several studies have examined the expression and putative activity of SGLT1 in mouse intestine (Lam et al. 2002; Hardcastle et al. 2004; Sandu et al. 2005). Additionally, work in multiple organisms, including mouse, has shown that expression of SGLT1 in the intestine is directly regulated by the sugar content of the diet (Solberg and Diamond 1987; Ferraris and Diamond 1993; Shirazi-Beechey et al. 1991; Dyer et al. 1997; Lescale-Matys et al. 1993). Mice also are a model organism in the study of the kidney, where SGLT1 is expressed in the proximal tubules (Breyer et al. 2007). However, despite abundant studies on mouse intestine and kidney SGLT1 proteins, the mouse homologue of SGLT1 has not been functionally characterized.

Very recently an X-ray crystal structure of SGLT from *Vibrio parahaemolyticus* (vSGLT) was published (Faham et al. 2008). The structure identifies the sugar binding site and predicts the Na^+ binding site. This structure includes transmembrane segment 1 (TM1) of vSGLT but the residues in TM1 were not assigned and the data do not suggest any specific role for this segment of the protein but do indicate that TM1 is not involved in ligand binding, nor does it form the translocation pathway.

Because of the widespread use of the mouse as a model organism and to fill the gap in knowledge surrounding the activity of a protein important to the function of the

intestine and the kidney, we cloned and biophysically characterized mouse SGLT1. Two different nucleotide sequences corresponding to mouse SGLT1 have previously been deposited, and the predicted primary structures of the proteins differ at amino acid 36 in TM1. The SGLT1 that we cloned from mouse kidney (mSGLT1) has a predicted amino acid sequence identical to one of those two deposited sequences (gi: 13277956), with a phenylalanine at position 36, while the alternate sequence (gi: 141802859) has a serine at this position.

Thus, to examine the role of the TM1 in SGLT1 function, and to determine whether the amino acid difference between the deposited mouse SGLT1 sequences results in altered protein activity, we mutated amino acid 36 in our cloned mSGLT1 to serine (F36S-mSGLT1) and functionally characterized both proteins. Our data establish that, like its homologues, mSGLT1 encodes a high-affinity Na^+/glucose cotransporter. In addition, we show that amino acid 36, and hence TM1, is involved in modulating the voltage dependence of protein function, and that any change in this voltage dependence will induce changes in a number of other functional characteristics, such as substrate affinity and turnover rate. Finally, our data provide a functional framework on which to interpret studies of glucose transport and regulation of SGLT1 expression and activity in mouse.

Experimental Procedures

Cloning of Mouse SGLT1

Full-length mouse SGLT1 cDNA was generated from 0.25 μg of mouse kidney poly(A)-RNA (Ambion) using oligo(dT) primers and Superscript III Reverse Transcriptase (Invitrogen). PCR was carried out with the following primers using Platinum *Taq* DNA Polymerase High Fidelity (Invitrogen): sense, 5′-ATG GAC AGT AGC ACC TTG AGC CCC-3′; and antisense, 5′-TCA GGC AAA ATA GGC ATG GCA GAA GAC-3′. The PCR product was cloned into the pCR2.1-TOPO vector using the TOPO-TA cloning kit (Invitrogen). mSGLT1 was then subcloned into the vector pCMV-Sport 6 for in vitro transcription and expression in oocytes.

Mutagenesis

The plasmid containing mSGLT1 cDNA was used as a template for site-directed mutagenesis. Phenylalanine at amino acid 36 was replaced by serine (F36S) using the QuikChange kit (Stratagene). The oligonucleotide primers used were as follows: F36S sense, 5′-TCG TCA TCT ACT CCG TGG TGG TGA T-3′; and F36S antisense, 5′-ATC ACC ACC ACG GAG TAG ATG ACG A-3′. The underlined letters represent the nucleotides changed. The gene was sequenced from start codon to stop codon to ensure that only the desired mutation was present.

Expression of Proteins in *Xenopus laevis* Oocytes

The mSGLT1 and F36S-mSGLT1 cDNAs were linearized with *Not*I and RNA was transcribed and capped in vitro using the SP6 RNA promoter (MEGAscript kit; Ambion). Mature *Xenopus laevis* oocytes were injected with 50 ng of cRNA coding for each protein. Oocytes were maintained in OR2 supplemented with penicillin (10,000 U/ml)/streptomycin (10 mg/ml) at 19°C for 1–3 days, until used.

Electrophysiology

Experiments were performed at room temperature using the two-electrode voltage-clamp method in a rapid perfusion chamber (Lostao et al. 1994). For experiments, oocytes were bathed in Na^+ buffer composed of (mM): 100 NaCl, 2 KCl, 1 $MgCl_2$, 1 $CaCl_2$, 10 Hepes/Tris, pH 7.4. In the Na^+-free buffer, choline-Cl replaced NaCl. The membrane potential was held at −50 mV and stepped for 100 ms from +50 to −150 mV in 20-mV decrements, or from 0 to −100 mV in 10-mV decrements. The sugar-dependent current was the difference between the current recorded in the sugar and the previous record in Na^+ buffer alone. Experiments were controlled and data were acquired using pClamp software (Axon Instruments).

The Na^+ apparent affinity ($K_{0.5}^{Na}$) was calculated using increasing Na^+ concentrations (0 to 100 mM) with 100 mM α-methyl-D-glucose (αMDG). The sugar apparent affinity ($K_{0.5}$) was obtained in 100 or 150 mM Na^+ with increasing sugar concentrations (0 to 10 mM). The steady-state currents at each membrane potential were fit with equation (1), $I = I_{max}[S]^n/(K_{0.5}^n + [S]^n)$, where I_{max} is the maximal current, [S] is the substrate concentration, $K_{0.5}$ is the substrate concentration for 0.5 I_{max}, and n is the Hill coefficient. For fitting of sugar dose-response curves n was set to 1.

Pre-Steady-State Currents

The charge movements measured with the voltage pulse ON and OFF are equal and opposite (Loo et al. 1993). The OFF currents were analyzed because the time constants are voltage independent, which makes the analysis more straightforward. Pre-steady-state (PSS) transient OFF currents were fit with double exponentials and the membrane capacitive component obtained from the fit was then subtracted from the current record, leaving the OFF currents

attributable to the transporter. The PSS transient charge, Q, was determined by integration of this transient OFF current with time, and the distribution of the charge moved as a function of membrane voltage (V) was calculated by fitting the data with a Boltzmann equation of the form

$$(Q - Q_{hyp})/Q_{max} = 1/\{1 + \exp[z(V - V_{0.5})F/RT]\}$$

where $Q_{max} = Q_{dep} - Q_{hyp}$ (Q_{dep} and Q_{hyp} are Q at depolarizing and hyperpolarizing limits, respectively), F is the Faraday constant, R is the gas constant, T is the absolute temperature, $V_{0.5}$ is the membrane potential where there is 50% charge transfer, and z is the apparent valence of the movable charge. Fits of data with equations were performed using SigmaPlot 9.0 (SPSS).

Uptake Experiments

αMDG uptake into oocytes was measured using a radioactive tracer technique (Ikeda et al. 1989). Oocytes were incubated in 50 μM αMDG with traces of ^{14}C-αMDG for 45 min in the presence or absence of 100 mM Na^+. The oocytes were then washed with cold Na^+-free solution and individually solubilized with SDS, and sugar uptake was determined using a scintillation counter. Sugar uptake in noninjected oocytes from the same batch of oocytes was used as control.

Results

We cloned SGLT1 from mouse kidney and studied the biophysical characteristics of the protein. Then we compared the characteristics of our cloned protein with the alternative protein predicted from the nucleotide database, which differs at amino acid 36 in TM1, outside of the ligand binding/translocation core.

Cloning of Mouse SGLT1

We cloned full-length SGLT1 cDNA from mouse kidney poly(A)-RNA (Swiss Webster) by reverse transcription and PCR. We found that the predicted amino acid sequence of our cloned cDNA was identical to one of two published sequences (gi: 13277956) and differed from the other (gi: 141802859). Specifically, at the nucleotide level, our clones contained thymidine at position 107 in all five colonies grown from the cloning reaction instead of cytidine (Fig. 1a). As a result, codon 36 (TTC) would translate as a phenylalanine, rather than a serine as is predicted from the alternate sequence. To determine whether this was due to a PCR artifact or to the mouse tissue or strain, additional reverse transcription and PCR reactions were performed with total RNA from kidney or small intestine extracted

A

```
5'-atggacagtagcaccttgagccccgcggttactgccaccgatgcacccatcccgtcc
   M  D  S  S  T  L  S  P  A  V  T  A  T  D  A  P  I  P  S
tacgagcgcattcgcaatgcggctgacatctcagtcatcgtcatctacttcgtggtggtg
   Y  E  R  I  R  N  A  A  D  I  S  V  I  V  I  Y  F  V  V  V
```

B

```
mouse          MDSSTLSPAVTATDAPIPSYERIRNAADISVIVIYFVVV 39
human          MDSSTWSPKTTAVTRPVETHELIRNAADISIIVIYFVVV 39
horse          MDSSTWSPGTATTAAPLASYERIRNAADISVIVIYFVVV 39
rat            MDSSTLSPAVTATDAPIQSYERIRNAADISVIVIYFVVV 39
cow            MDSSTWSPPATATAEPLPPYERIRNAADISVIVIYFVVV 39
sheep          MDSSTWSPPATATAEPLQAYERIRNAADISVIVIYFVVV 39
dog            MDSTTWSPMTNATASPLAPHERIRNAADISVIVIYFVVV 39
rabbit         MDSSTLSPLTTSTAAPLESYERIRNAADISVIVIYFLVV 39
               *** * **       *    * ******** ***** **
```

Fig. 1 **a** Nucleotide and amino acid sequences of mouse SGLT1 cDNA. **b** Amino acid alignment of the N-terminal part of SGLT1 proteins. Amino acid 36 is shown in boldface. *Residues in that column are identical in all sequences in the alignment. Mouse, gi: 13277956; human, gi: 4507031; horse, gi: 126352558; rat, gi: 6981552; cow, gi: 27807095; sheep, gi: 62821778; dog, gi: 55741754; rabbit, gi: 127805

from different strains of mice. We repeated RT-PCR reactions with total RNA from intestine from mouse strain 129/ReJ (a gift from Dr. Nirupa Chaudhari) and from both kidney and intestine from a third mouse (a cross between B6.Cg-TgN[SOD1-G93A]1Gur/J and B6.Cg-Tg[Thy1-YFP]16Jrs/J; a gift from Dr. Ellen Barrett). In every case thymidine was found at nucleotide 107. In this paper, we name the protein coded by the cDNA we cloned mSGLT1, and the alternate protein predicted from the database F36S-mSGLT1. Figure 1b shows an amino acid alignment of several cloned SGLT1 proteins which illustrates that amino acid 36 is conserved as phenylalanine.

Sugar Uptake

To study the functionality of mSGLT1, we expressed the protein in *X. laevis* oocytes and measured radiolabeled sugar uptake for 45 min. αMDG uptake experiments were done in noninjected oocytes (control), oocytes expressing mSGLT1, and oocytes expressing F36S-mSGLT1. Figure 2a shows that expression of either protein increased αMDG uptake with respect to control oocytes (0.04 ± 0.003 pmol/min) and that the sugar uptake in mSGLT1 (5.6 ± 0.4 pmol/min) was higher than the uptake in F36S-mSGLT1 (3.4 ± 0.3 pmol/min). In addition, we established that the uptake was Na^+ dependent by performing the same experiment in Na^+-free solution. Under this condition, the uptake values were much lower: 0.02 ± 0.005, 0.2 ± 0.06, and 0.04 ± 0.01 pmol/min in noninjected, mSGLT1, and F36S-mSGLT1, respectively. Uptakes after 45 min were still in the linear range.

Figure 2b shows 50 mM αMDG-induced current in mSGLT1 and F36S-mSGLT1 at voltages ranging from +50 to −150 mV. mSGLT1 shows a higher sugar-induced current at every voltage.

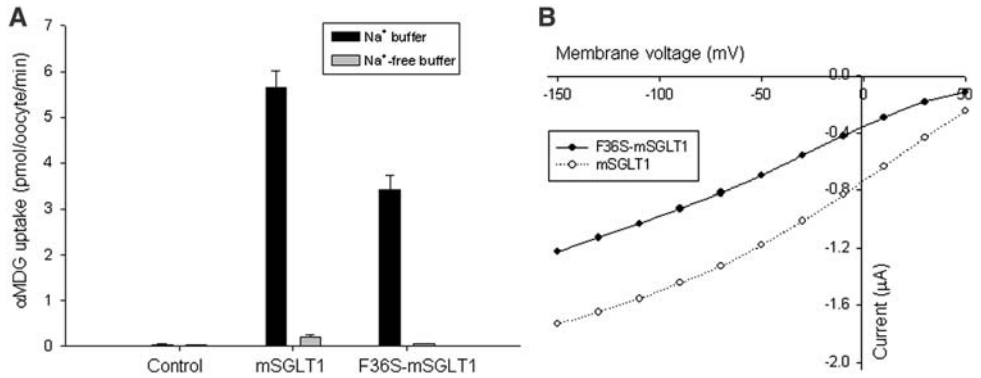

Fig. 2 **a** Sugar uptake experiments. Uptake of 50 μM αMDG in control oocytes (noninjected) and oocytes expressing mSGLT1 or F36S-mSGLT1 in the presence or absence of Na^+. Data represent picomoles αMDG uptake per minute by individual cells and are shown as mean ± SE; n = 4–7 oocytes. **b** Steady-state current/voltage curves for mSGLT1 and F36S-mSGLT1: 50 mM αMDG-induced currents were measured in the presence of Na^+ at voltages ranging from +50 to −150 mV in oocytes expressing each of the proteins

Na^+ and Sugar Apparent Affinities

To characterize the biophysical properties of the two proteins, we calculated their apparent affinities for Na^+ ($K_{0.5}^{Na}$) and sugar ($K_{0.5}$). $K_{0.5}^{Na}$ values were obtained at different voltages by measuring sugar-induced currents in saturated αMDG (100 mM) with Na^+ concentrations ranging from 1 to 100 mM. Figure 3a shows representative data from one oocyte obtained at −50 mV, represented as percentage maximal current in one mSGLT1 (open circles)- and one F36S-mSGLT1 (filled circles)-expressing oocyte. Data were fitted with the Hill equation (solid lines) and showed that $K_{0.5}^{Na}$ values were different for the two proteins. In the example shown in Fig. 3a, the Na^+ apparent affinity for one mSGLT1-expressing oocyte was 6 ± 0.3 mM, while for F36S-mSGLT1 it was 13 ± 0.6 mM. The Hill coefficient (*n*) was the same for both proteins. Figure 3b shows the mean $K_{0.5}^{Na}$ for five different oocytes for each protein at different voltages. It shows the voltage dependence of the $K_{0.5}^{Na}$ for both mSGLT1 and F36S-mSGLT1, demonstrating that the $K_{0.5}^{Na}$ values were higher at depolarizing voltages in both proteins. Moreover, at every tested voltage (from −100 to 0 mV) the $K_{0.5}^{Na}$ value was lower in mSGLT1 than in F36S-mSGLT1.

Next, we examined the apparent affinities and maximal currents for three sugars. Glucose, αMDG, and galactose $K_{0.5}$ values were calculated by measuring sugar-induced currents with different concentrations of each sugar in 100 mM Na^+. Figure 4a shows glucose (open circles)- and galactose (solid circles)-induced currents in one mSGLT1-expressing oocyte at −100 mV. Each data set was fitted with equation (1) (lines), showing that the $K_{0.5}$ was 0.28 ± 0.02 mM for glucose but 1.3 ± 0.04 mM for galactose. αMDG $K_{0.5}$ was also obtained in the same oocyte, with the value of 0.96 ± 0.1 mM (not shown). Furthermore, we studied whether the substitution of residue 36 would modify the sugar affinities. Thus, we determined the $K_{0.5}$ of the three sugars in oocytes expressing F36S-mSGLT1. Figure 4b shows average $K_{0.5}$ values, at

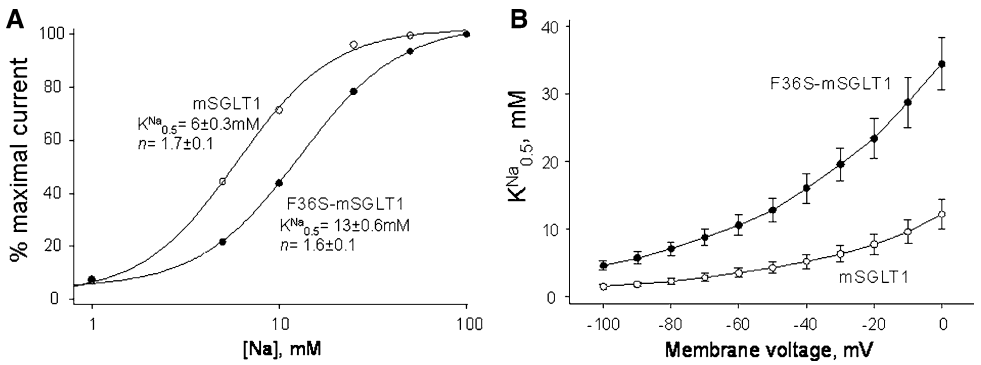

Fig. 3 Apparent Na^+ affinity of mSGLT1 and F36S-mSGLT1. **a** Na^+ affinity at −50 mV. Induced currents in representative oocytes expressing mSGLT1 and F36S-mSGLT1 at Na^+ concentrations ranging from 0 to 100 mM, while the sugar (αMDG) was maintained at a saturated concentration (100 mM). Currents were normalized to the maximal value in each oocyte. Data were fitted with a Hill equation to obtain the $K_{0.5}^{Na}$ values and Hill coefficient values (*n*). **b** Na^+ apparent affinities in mSGLT1 and F36S-mSGLT1 (n = 5) at voltages ranging from −100 to 0 mV. Data are mean ± SE

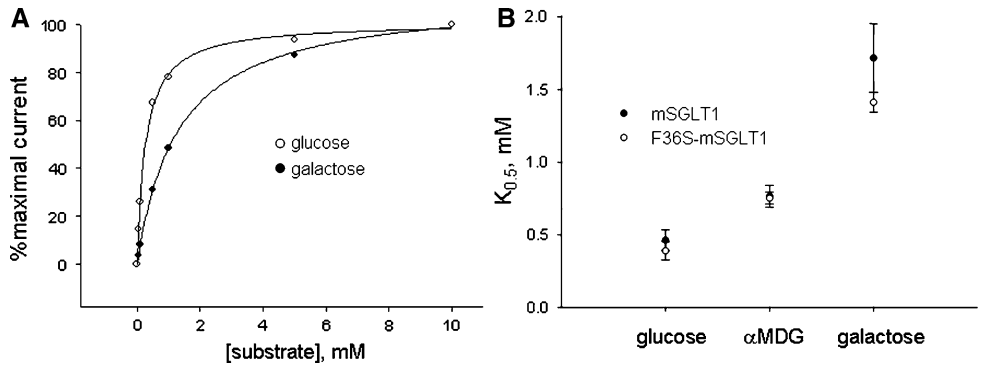

Fig. 4 Apparent sugar affinities measured at −100 mV. **a** Apparent affinity for glucose and galactose of one representative oocyte expressing mSGLT1. The data were fitted (solid lines) with equation (1) to estimate $K_{0.5}$ values for each sugar tested: glucose, $K_{0.5} = 0.3 \pm 0.02$ mM; and galactose, $K_{0.5} = 1.3 \pm 0.04$ mM. **b** Average $K_{0.5}$ values in mSGLT1 and F36S-mSGLT1 for glucose, αMDG, and galactose

−100 mV, for glucose (n = 6–7), αMDG (n = 7–8), or galactose (n = 7–10) obtained from oocytes expressing mSGLT1 or F36S-mSGLT1. The averaged data showed similar results to the single oocyte experiment (Fig. 4a); glucose had the highest apparent affinity, followed by αMDG and then galactose. Maximal currents (I_{max}) induced by the three sugars were voltage dependent, with maximal currents at hyperpolarizing voltages. The I_{max} for glucose, galactose, and αMDG in mSGLT1 were very similar at every voltage (−100 to 0 mV), and the same was observed in F36S-mSGLT1. However, I_{max} values were higher in mSGLT1 than in F36S-mSGLT1 at every voltage, as shown in Fig. 2b for αMDG.

Since sugar affinity is voltage dependent in SGLT proteins, we determined αMDG $K_{0.5}$ values at voltages ranging from 0 to −100 mV, in mSGLT1 and F36S-mSGLT1. Figure 5a shows that in mSGLT1, αMDG $K_{0.5}$ values (open circles) were higher at depolarizing voltages, indicating that the apparent affinity for the sugar was lower when the membrane potential was more positive. In F36S-mSGLT1, αMDG $K_{0.5}$ values (solid circles) were also voltage dependent; however, the voltage dependence was greater than in mSGLT1. Therefore, although mSGLT1 and F36S-mSGLT1 αMDG apparent affinities at −100 mV were the same (Fig. 4b), at more depolarizing voltages the F36S-mSGLT1 apparent affinities were lower than the mSGLT1 affinities. Figure 3b shows that the Na^+ affinities were lower in F36S-mSGLT1 than in mSGLT1, and that they were also voltage dependent. Is the greater voltage dependence of the sugar affinity in F36S-mSGLT1 a consequence of the different Na^+ affinities? When determining αMDG apparent affinities of F36S-mSGLT1 (Fig. 5a), the concentration of Na^+ in the medium was 100 mM. Consequently, Na^+ could be limiting at depolarizing voltages in the F36S-mSGLT1 transport turnover rate (Fig. 3b). To address this question, we calculated the αMDG $K_{0.5}$ in 150 mM Na^+, so the Na^+ concentration would be less likely to limit the protein turnover rate. Figure 5b shows that in 150 mM Na^+, αMDG $K_{0.5}$ values for F36S-mSGLT1 trended toward higher affinity at voltages more depolarized

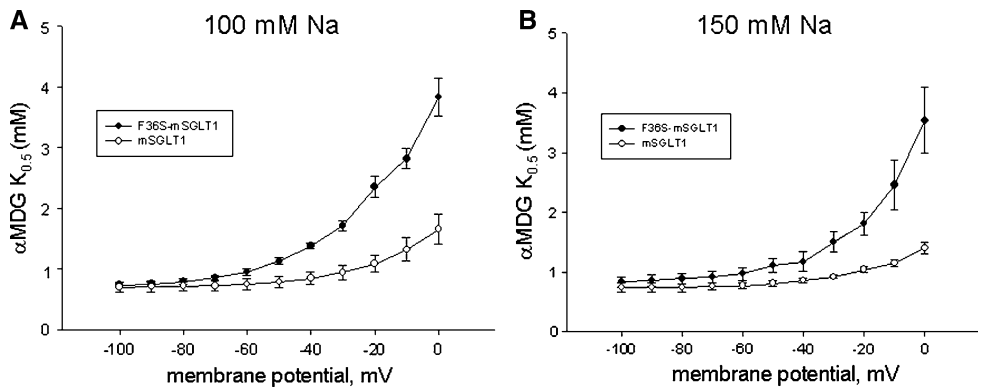

Fig. 5 αMDG affinity in mSGLT1 and F36S-mSGLT1. **a** αMDG affinities in buffer containing 100 mM Na^+ at voltages ranging from 0 to −100 mV in mSGLT1 (n = 6; open symbols) and in F36SmSGLT1 (n = 7; filled symbols). **b** αMDG affinities in both proteins in buffer containing 150 mM Na^+ (mSGLT1, n = 3; F36S-mSGLT1, n = 5). Data are mean ± SE

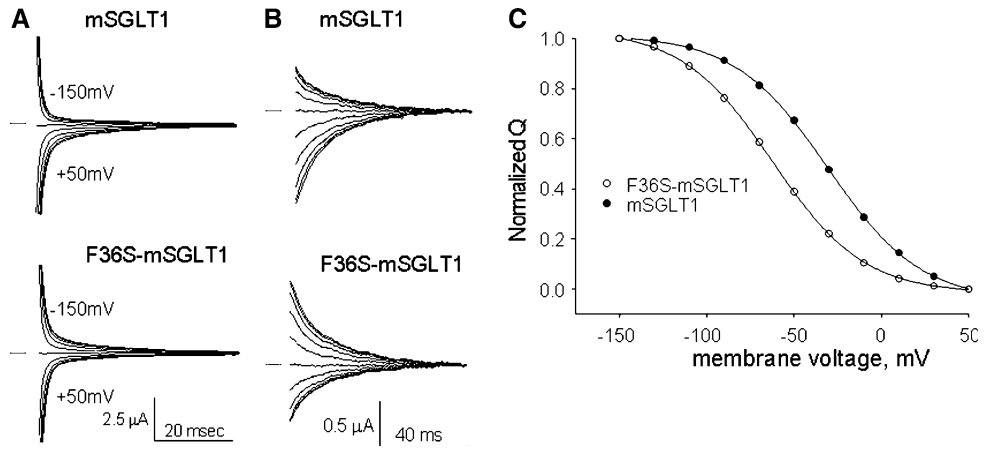

Fig. 6 Comparison of pre-steady-state currents of mSGLT1 with F36S-mSGLT1. **a** The membrane voltage was held at −50 mV and stepped for 100 ms from +50 to −150 mV, in 20-mV increments (not shown). Then the membrane voltage was returned to −50 mV for 100 ms (shown). These graphics show the characteristics of the Na^+-dependent OFF currents, which show the total current record containing the membrane bilayer capacitive transient, the pre-steady-state current, and the steady-state current. **b** Pre-steady-state OFF-current traces for both proteins were obtained by subtracting the membrane bilayer capacitive transient component and the steady-state current from the total currents shown in **a**. The charge transfer was obtained by integrating the compensated transient currents at each potential with respect to time. **c** Charge/voltage relationships of representative mSGLT1- and F36S-mSGLT1-expressing oocytes (same cells presented in **a** and **b**) at membrane voltage varying from +50 to −150 mV. The solid lines are the fit of the data to the Boltzmann equation, which show that mSGLT1 and F36S-mSGLT1 have different $V_{0.5}$ values (−31 and −62 mV, respectively)

than −40 mV. Although these changes were not significant, they suggest that Na^+ apparent affinity may be, at least in part, responsible for the differences in sugar apparent affinity. Attempts to increase the Na^+ concentration further resulted in unstable recordings and dead cells over the relatively long time course of the experiment.

Pre-Steady-State Analysis

In the absence of sugar, SGLT1 proteins exhibit a PSS current after a step change in membrane voltage. These currents are generally attributed to voltage-dependent changes in the conformation of the transporter (Parent et al. 1992; Loo et al. 2006; Birnir et al. 1991). To analyze the PSS records, oocytes expressing mSGLT1 or F36S-mSGLT1 were clamped at −50 mV and the voltage was then stepped for 100 ms from +50 to −150 mV in 20-mV decrements (ON currents). Then the membrane voltage returned to −50 mV for 100 ms (OFF currents). For all voltage pulses, the transient currents rapidly decayed to a steady state. Figure 6a shows representative OFF currents of one mSGLT1- and one F36S-mSGLT1-expressing oocyte. These raw current traces already showed that the PSS currents in the proteins differ from one another. To determine how the PSS currents vary, we analyzed those currents. At each voltage the charge movement (Q) was obtained by separating the membrane capacitance and the steady-state conductances and by integrating the transient currents (Fig. 6b), which further illustrated the differences between the distributions of the two proteins in different states. We plotted the charge at each voltage (Q/V) and obtained a sigmoid curve that we fit with the Boltzmann equation. The fit gave us the maximal charge transfer, Q_{max}, as the difference between Q at depolarizing limits and Q at hyperpolarizing limits, which is proportional to the number of transporters in the membrane of the cell. The similar Q_{max} in mSGLT1 (29 ± 2 nC; n = 4) and F36S-mSGLT1 (30 ± 1 nC; n = 4) indicates that the expression levels of both proteins are the same ($p > 0.5$) given that the estimated charge is the same in both proteins, z = 1. $V_{0.5}$ values, also obtained from the fits, indicated that the distribution of the proteins differ significantly: −30 ± 1 mV

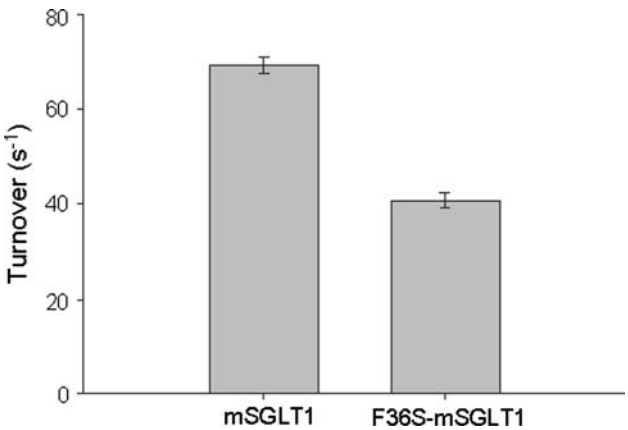

Fig. 7 Turnover rate was calculated with currents obtained at −150 mV with saturating Na^+ and sugar (10 mM αMDG and 100 mM Na^+). The numbers are 70 ± 2 per second for mSGLT1 (n = 4) and 40 ± 2 per second for F36S-mSGLT1 (n = 4)

for mSGLT1 (n = 4) and −61 ± 1 mV for F36S-mSGLT1 (n = 4; $p < 0.0001$).

Turnover Number

To calculate the apparent turnover number of each protein, we used the total amount of SGLT1 in the oocyte membrane, estimated from Q_{max}, and the maximal sugar-induced current obtained in each oocyte at −150 mV in saturating sugar (10 mM αMDG). The I_{max} values were 1960 ± 140 and 1200 ± 50 nA for mSGLT1 and F36S-mSGLT1, respectively. The turnover numbers (Fig. 7) of mSGLT1 and F36S-mSGLT1 were 70 ± 2 and 40 ± 2 per second, indicating that mSGLT1 cycled faster than F36S-mSGLT1.

Discussion

Two nucleotide sequences have been deposited for mouse SGLT1, which differ at base 107 (thymidine vs cytidine), thus changing the amino acid composition of the protein. Other base differences between the two sequences are silent. In this study, we cloned the full-length SGLT1 cDNA from three different mouse strains and obtained a sequence whose translated amino acid sequence was identical to one of the deposited sequences (gi: 13277956), with a thymidine at position 107 (Fig. 1a) that results in a phenylalanine at amino acid 36, which is located in TM1 based on the crystal structure of vSGLT (Faham et al. 2008). Similarly, Tabatabai et al. (2001) also sequenced mouse SGLT1 cloned from kidney and identified a phenylalanine at amino acid 36. In addition, amino acid alignment of SGLT1s from numerous species (Fig. 1b) shows that phenylalanine is conserved among all these proteins. These data suggest that mouse SGLT1 contains a phenylalanine at amino acid 36. Further experiments will be required to determine whether the alternative sequence (gi: 141802859) represents a natural polymorphism at this position.

The recent crystal structure provides a wealth of information about the binding of ligands and potential mechanisms for the transport of sugars by SGLT proteins (Faham et al. 2008). However, it has comparatively little to say about the potential contributions of transmembrane segments outside of the "core" TM segments. To examine the contribution of TM1 toward the function of SGLT1, we have taken advantage of the *Xenopus laevis* oocyte system to express and characterize mSGLT1 and F36S-mSGLT1. Our uptake experiments clearly revealed sodium-dependent sugar transport (Fig. 2). Notably, sugar uptake in mSGLT1-expressing oocytes was higher than in F36S-mSGLT1-expressing ones. Nevertheless, at a qualitative level mSGLT1 and F36S-mSGLT1 both recapitulate the function as a Na^+/sugar cotransporter previously demonstrated for human, rat, rabbit, and *Vibrio* homologues.

The apparent Na^+ affinities differ between mSGLT1 and F36S-mSGLT1. Na^+ affinity in mSGLT1 is twice as strong as in F36S-mSGLT1. vSGLT has only one Na^+ binding site, which is likely to be conserved in other SGLT homologues (Faham et al. 2008). The location of the second Na^+ binding site for SGLT1 proteins is unknown. The crystal structure of LueT (Yamashita et al. 2005) shows two Na^+ binding sites, one between TM1 and TM6, where the leucine also binds, and the other between TM1 and TM8. Mutagenesis of vSGLT and structural alignment with LeuT suggest that the vSGLT Na^+ binding site between TM2 and TM9 is structurally equivalent to the LeuT site between TM1 and TM8. Notably, TM1 in vSGLT contacts TM9 and any changes in the sequence of TM1 could alter the helical packing and subsequently alter the affinity for the adjacent Na^+ binding site. Such a mechanism could contribute to the altered Na^+ affinity seen in F36S-mSGLT1. Likewise, it suggests that transmembrane segments outside of the translocation pathway and ligand binding sites are critical for maintaining the contacts necessary for efficient transport and that mutations in these segments may have broad effects on the protein function.

Both clones of mouse SGLT1 showed different apparent affinities for glucose compared to αMDG or galactose. In contrast, human SGLT1 (hSGLT1) has the same affinity for these three sugars (Díez-Sampedro et al. 2000). In mSGLT1 the biggest difference in affinities is between galactose and glucose. These two sugars differ only in the orientation of the –OH group of C4. The results indicate that the axial orientation in galactose decreases the affinity for mSGLT1 compared to the equatorial orientation in glucose. This suggests that, although mSGLT1 and hSGLT1 have high amino acid identity (88%), one or several of the different amino acids in mSGLT1 makes the galactose interaction with the protein weaker. The crystal of vSGLT identified five residues that interact with the sugar. Among these, mSGLT1 and hSGLT1 differ only at residue 287 (A in mSGLT1 and T in hSGLT1). Intestingly, the sugar interacts with this amino acid through the –OH group of C4 (Faham et al. 2008), explaining the difference in selectivity for galactose between hSGLT1 and mSGLT1.

As reported for other Na^+/glucose cotransporters, the apparent affinity for sugar depends on the membrane voltage. We found that the apparent affinity of mSGLT1 for αMDG changed from ~0.75 to ~1.5 mM as the membrane potential changed from −100 to 0 mV. This behavior is shared with both human and rat SGLT1 (Panayotova-Heiermann et al. 1995; Hirayama et al. 1996), while rabbit SGLT1 (Birnir et al. 1991) appears to be the lone member of the family with only weakly voltage sensitive apparent sugar affinity. Table 1 compares steady-

Table 1 Steady-state and pre-steady-state kinetic parameters of rabbit, human, rat, and mouse Na^+/glucose cotransporters

SGLT1	$K_{0.5}^{Na}$ (mM)	$K_{0.5}$ αMDG (mM)	Q_{max} (nC)	z	$V_{0.5}$ (mV)	I_{max}/Q_{max}
Rabbit[a]	14	0.15	80	1	+0.5	25
Human[b,c]	26	0.45	20	1	−39	57
Rat[d]	26	0.3	10	1	−43	30
Mouse	6	0.8	29	1	−30	69

Note: Na^+ and sugar apparent affinity values were obtained at −50 mV. Sources: [a] Panayotova-Heiermann et al. (1994); [b] Loo et al. (1993); [c] Hirayama et al. (1996); [d] Panayotova-Heiermann et al. (1995)

state and PSS kinetic parameters for rabbit, rat, human, and mouse Na^+/glucose cotransporters.

F36S-mSGLT1 showed greater voltage sensitivity in sugar apparent affinity than did mSGLT1 (Fig. 5). This greater voltage sensitivity could be explained, at least in part, by decreased Na^+ occupancy at depolarized potentials (Fig. 3). As discussed by Hirayama et al. (1991), since Na^+ is essential, decreased occupancy of the Na^+ binding sites would result in a decreased apparent affinity for sugar. In both clones at hyperpolarized potentials (<−60 mV), the apparent affinity for Na^+ is below 10 mM (Fig. 3b). Thus, the transporter should be saturated by the 100 mM Na^+ present during the experiment. At these potentials mSGLT1 and F36S-mSGLT1 have the same apparent affinity for αMDG (Fig. 5a). However, at more depolarized potentials the decrease in apparent affinity for Na^+ in F36S-mSGLT1 would result in the decrease in the apparent affinity for sugar. To investigate this we increased the Na^+ concentration to 150 mM and reassessed the apparent sugar affinity. The αMDG $K_{0.5}$ values of mSGLT1 and F36S-mSGLT1 were now similar up to −40 mV. In 150 mM Na^+, we found a small, though not significant, change in the apparent sugar affinities at all voltages more depolarized than −40 mV. Figure 3b shows that the apparent affinity F36S-mSGLT1 for Na^+ at −40 mV was close to 15 mM, suggesting that at more depolarizing voltages, the Na^+ binding sites will not be saturated, even in 150 mM Na^+. This could explain why at voltages more depolarized than −40 mV, the sugar apparent affinity difference between mSGLT1 and F36S-mSGLT1 is still present. Because of the effects of increases in osmolarity, we could not increase the Na^+ concentration further. Nevertheless, it is likely that the differences in sugar affinity between apparent mSGLT1 and F36S-mSGLT1 could be a consequence, at least in part, of their different Na^+ affinities.

PSS currents were first studied in rabbit SGLT1 (Parent et al. 1992; Birnir et al. 1991). PSS currents represent conformational changes that occur in the protein in response to the presence of Na^+ or changes in membrane potential and are associated with reorientation of the empty

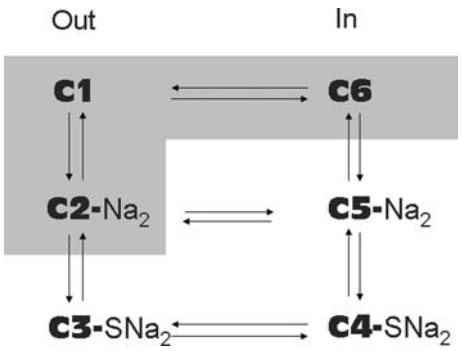

Fig. 8 Scheme of the simplified six-state kinetic model for Na^+/glucose cotransport (modified from Loo et al. 1993). States C1, C2, and C3 face the external membrane surface. In the absence of ligands, the transporter exists in states C1 and C6. At the external surface 2 Na^+ ions bind to the transporter (C2). Then sugar (S) binds (C3) and there is another change to C4 that transports sugar and Na^+. Pre-steady-state currents are hypothesized to be due to partial reactions among C2-C1-C6 (shaded area)

transporter from one side of the membrane to the other and binding/dissociation of the Na^+ to the protein on the external membrane surface. In terms of the commonly used six-state kinetic model to describe SGLT1 activity (Fig. 8), these correspond to the movements between C1–C6 (reorientation of the empty protein between the external and the internal facing conformations) and C1–C2 (binding and dissociation of Na^+ to the protein), shown shaded in Fig. 8 (Parent et al. 1992; Loo et al. 1993, 1998).

As in other SGLT1 proteins, PSS currents in mSGLT1 are suppressed in the presence of sugar or the absence of Na^+ (not shown). Because the PSS currents report on movement of the transporter, the charge-voltage curve (Q-V; Fig. 6c) is indicative of the distribution of the empty transporter between inward (C6)- and outward-facing conformations as well as binding (C2)/unbinding (C1) of Na^+ to the transporter. For mSGLT1 the $V_{0.5}$, the voltage where the transporter is equally distributed between C1 and C6, is −36 mV. This is between the $V_{0.5}$ values previously established for hSGLT1, −39 mV (Loo et al. 1993), and rabbit SGLT1, 0 mV (Panayotova-Heiermann et al. 1994). Mutating a single amino acid in rabbit SGLT1 resulted in a hyperpolarizing shift in the $V_{0.5}$ (Panayotova-Heiermann et al. 1994). Similarly, a single amino acid difference in the mouse SGLT1, F36S-mSGLT1, results in a shift in $V_{0.5}$ to significantly more hyperpolarized potentials (−62 mV) (Fig. 6c). These data indicate that mutating the side chain at position 36 results in a redistribution of the protein, favoring the inward-facing conformation (C6) at rest. Viewed in terms of the six-state kinetic model, the mutation would result in a change in the rate constant between C6 and C1. The result of this altered rate constant would be a decrease in the apparent affinity for Na^+, as we found in Fig. 3. Thus, alterations of TM1 can contribute to the decreased apparent affinity for

Na^+ both through a difference in packing of TM segments adjacent to the site and through a redistribution of the protein to an inward-facing conformation.

In our experiments, we noted that oocytes expressing mSGLT1 took up sugar faster than F36S-mSGLT1 (Fig. 2). In addition to the higher uptake rate, maximal sugar-induced currents (I_{max}) in mSGLT1 were higher than in F36S-mSGLT1 (Fig. 2b). This difference in activity could be due to several factors, including altered functional properties (such as a different affinity for substrates) and differences in the level of surface expression. To examine this second possibility, we measured the Q_{max} from the PSS analysis for each of the two proteins. Q_{max} is a measure of the maximum charge movement and, given equivalent charge movement per transporter, has been shown to correlate with the level of surface expression of SGLT1 (Loo et al. 1993). Our experiments showed both that the charge moved per transporter was equal and that there was no difference in Q_{max} between mSGLT1 and F36S-mSGLT1, suggesting that the clones are expressed equally well. Thus, differences in sugar uptake are due to functional differences between the proteins, including changes in Na^+ and/or sugar affinity (which may in turn be due to differences in the voltage dependence of the proteins), but are not due to changes in expression levels.

Finally, we measured the turnover number for both proteins in saturating Na^+ and αMDG by dividing the maximal current in αMDG (I_{max}) by the Q_{max} (Loo et al. 1993). This analysis reveals that the turnover number was 69 s^{-1} for mSGLT1 but only 41 s^{-1} for F36S-mSGLT1, a decrease of 40% (Fig. 7). This decrease in turnover caused by the change of residue 36 is expected to decrease the rate of sugar transport and, along with the differences in apparent sugar (and Na^+) affinities, is likely the cause of the differences in activity seen between the two clones. For comparison, the turnover number for human SGLT1 is 57 s^{-1} (Loo et al. 1993).

In conclusion, we have demonstrated that mSGLT1 behaves as a high-affinity Na^+/sugar cotransporter similar in characteristics to SGLT1 proteins from other species. We have shown that TM1, despite its location away from the "core" and its not directly binding Na^+ or sugar, or taking part in the translocation pathway, exerts significant effects on the apparent substrate affinities and voltage sensitivity of the protein. This voltage sensitivity is a consequence of a conformational redistribution that favors the inward-facing conformation. Finally, we show that these functional changes directly affect the efficiency with which the protein transports sugar into cells.

Acknowledgments I thank Rebekah Denison for technical assistance and E. M. Wright, B. A. Hirayama, D. D. Loo, C. Grewer, and P. Larsson for comments and suggestions on the manuscript.

References

Birnir B, Loo DD, Wright EM (1991) Voltage-clamp studies of the Na^+/glucose cotransporter cloned from rabbit small intestine. Pflugers Arch 418:79–85

Breyer MD, Tchekneva E, Qi Z, Takahashi T, Fogo AB, Harris RC (2007) Examining diabetic nephropathy through the lens of mouse genetics. Curr Diab Rep 7:459–466

Díez-Sampedro A, Lostao MP, Wright EM, Hirayama BA (2000) Glycoside binding and translocation in Na(+)-dependent glucose cotransporters: comparison of SGLT1 and SGLT3. J Membr Biol 176:111–117

Dyer J, Hosie KB, Shirazi-Beechey SP (1997) Nutrient regulation of human intestinal sugar transporter (SGLT1) expression. Gut 41:56–59

Faham S, Watanabe A, Besserer GM, Cascio D, Specht A, Hirayama BA, Wright EM, Abramson J (2008) The crystal structure of a sodium galactose transporter reveals mechanistic insights into Na^+/sugar symport. Science 321:810–814

Ferraris RP, Diamond JM (1993) Crypt/villus site of substrate-dependent regulation of mouse intestinal glucose transporters. Proc Natl Acad Sci USA 90:5868–5872

Hardcastle J, Harwood MD, Taylor CJ (2004) Absorption of taurocholic acid by the ileum of normal and transgenic DeltaF508 cystic fibrosis mice. J Pharm Pharmacol 56:445–452

Hirayama BA, Wong HC, Smith CD, Hagenbuch BA, Hediger MA, Wright EM (1991) Intestinal and renal Na^+/glucose cotransporters share common structure. Am J Physiol 261:C296–C304

Hirayama BA, Lostao MP, Panayotova-Heiermann M, Loo DD, Turk E, Wright EM (1996) Kinetic and specificity differences between rat, human, and rabbit Na^+-glucose cotransporters (SGLT–1). Am J Physiol 270:G919–G926

Ikeda TS, Hwang ES, Coady MJ, Hirayama BA, Hediger MA, Wright EM (1989) Characterization of a Na^+/glucose cotransporter cloned from rabbit small intestine. J Membr Biol 110:87–95

Kimmich GA (1981) Intestinal absorption of sugar. In: Johnson LR (ed) Physiology of the gastrointestinal tract. Raven Press, New York

Lam MM, O'Connor TP, Diamond J (2002) Loads, capacities and safety factors of maltase and the glucose transporter SGLT1 in mouse intestinal brush border. J Physiol 542:493–500

Lescale-Matys L, Dyer J, Scott D, Freeman TC, Wright EM, Shirazi-Beechey SP (1993) Regulation of the ovine intestinal Na +/glucose co-transporter (SGLT1) is dissociated from mRNA abundance. Biochem J 291:435–440

Loo DD, Hazama A, Supplisson S, Turk E, Wright EM (1993) Relaxation kinetics of the Na^+/glucose cotransporter. Proc Natl Acad Sci USA 90:5767–5771

Loo DD, Hirayama BA, Gallardo EM, Lam JT, Turk E, Wright EM (1998) Conformational changes couple Na^+ and glucose transport. Proc Natl Acad Sci USA 95:7789–7794

Loo DD, Hirayama BA, Karakossian MH, Meinild AK, Wright EM (2006) Conformational dynamics of hSGLT1 during Na^+/glucose cotransport. J Gen Physiol 128:701–720

Lostao MP, Hirayama BA, Loo DD, Wright EM (1994) Phenylglucosides and the Na^+/glucose cotransporter (SGLT1): analysis of interactions. J Membr Biol 142:161–170

Panayotova-Heiermann M, Loo DD, Lostao MP, Wright EM (1994) Sodium/D-glucose cotransporter charge movements involve polar residues. J Biol Chem 269:21016–21020

Panayotova-Heiermann M, Loo DD, Wright EM (1995) Kinetics of steady-state currents and charge movements associated with the rat Na^+/glucose cotransporter. J Biol Chem 270:27099–27105

Parent L, Supplisson S, Loo DD, Wright EM (1992) Electrogenic properties of the cloned Na^+/glucose cotransporter. I. Voltage-clamp studies. J Membr Biol 125:49–62

Sandu C, Rexhepaj R, Grahammer F, McCormick JA, Henke G, Palmada M, Nammi S, Lang U, Metzger M, Just L, Skutella T, Dawson K, Wang J, Pearce D, Lang F (2005) Decreased intestinal glucose transport in the sgk3-knockout mouse. Pflugers Arch 451:437–444

Shirazi-Beechey SP, Hirayama BA, Wang Y, Scott D, Smith MW, Wright EM (1991) Ontogenic development of lamb intestinal sodium-glucose co-transporter is regulated by diet. J Physiol 437:699–708

Solberg DH, Diamond JM (1987) Comparison of different dietary sugars as inducers of intestinal sugar transporters. Am J Physiol 252:G574–G584

Tabatabai NM, Blumenthal SS, Lewand DL, Petering DH (2001) Differential regulation of mouse kidney sodium-dependent transporters mRNA by cadmium. Toxicol Appl Pharmacol 177:163–173

Yamashita A, Singh SK, Kawate T, Jin Y, Gouaux E (2005) Crystal structure of a bacterial homologue of Na^+/Cl^- dependent neurotransmitter transporters. Nature 437:215–223